

# Generating highly entangled states via discrete-time quantum walks with Parrondo sequences

B. Varun Govind<sup>1,\*</sup> and Colin Benjamin<sup>1,†</sup>

<sup>1</sup>*School of Physical Sciences, National Institute of Science Education and Research, HBNI, Jatni 752050, India*

Quantum entanglement has multiple applications in quantum information processing. Methods to generate highly entangled states independent of initial conditions is an essential task. Herein we aim to generate highly entangled states via discrete time quantum walks. We propose deterministic Parrondo sequences that generate states that are, in general, much more entangled than states produced by sequences using only either one of the two coins. We show that some Parrondo sequences generate highly entangled states which are independent of the phase of the initial state used and further lead to maximally entangled states in some cases. We study Parrondo sequences for both small number of time steps as well as the asymptotic limit of a large number of time steps.

## I. INTRODUCTION

Parrondo's paradox involves two losing games A and B which when combined produces a winning outcome. These were introduced as a pedagogical illustration of the Brownian ratchet[1] and has spawned significant interest across diverse fields ever since[2, 3]. Parrondo's concept has been extended into other potential applications[2] and has been customized to explain many physical and biological processes and their functioning[4]. The quantum version of the paradox was introduced in Refs. [5, 6]. Quantum walks, were introduced in [7] and are a sophisticated tool for designing quantum algorithms [8]. Apart from uses in quantum computation, quantum walks have been used to explain, control, and simulate the dynamics in various complex physical systems[8]. Further, quantum walks can be directly implemented in labs without using a quantum computer[8]. Quantum walks have already been realized in ultra-cold rubidium-87 atoms[9], photons[10, 11], neutral atoms[12], NMR quantum-information processors[13], superconducting qubits[14, 15] and trapped ions[16, 17]. In a discrete-time quantum walk(DTQW), each step takes exactly a one-time unit. DTQW's allow for the exploration of numerous non-trivial geometric and topological phenomena[18] and multi-path quantum interference[19]. DTQW's are characterized by an evolution which consists of repeated application of two operators, the coin operator, and the shift operator. Parrondo's paradox has been explored several times using one-dimensional DTQW's[5, 6, 20, 21]. It was shown that instead of a single coin if a two-coin initial state is considered, Parrondo's paradox can be observed in quantum walks even in the asymptotic limits[22], and further replacing a two-state coin(qubit) with a three state coin(qutrit) also leads to Parrondo's paradox in asymptotic limits[23].

A renewed interest in exploiting DTQW's as a tool to generate entanglement has been reported recently. In this

context, developing faster methods to generate entanglement which are also experimentally feasible is an important task of current research. A particular and intriguing way is via hybrid entanglement. Hybrid entanglement as the name suggests is the entanglement between different degrees of freedom like polarization, orbital angular momentum, time-bin energy, or spatial mode. If these degrees of freedom belong to the same particle, more information can be encoded at the single-particle level, which can help to reduce the required resources [24]. Photonic hybrid entangled states can be advantageous in optical quantum networks as it enables a more flexible network with each photon being transmitted through the more suited channel [25]. Photonic quantum information offers several technological applications [26]. Photonic implementations of discrete-time quantum walk have been explored several times[25]. In this scenario, the preparation of maximally hybrid entangled states using DTQWs is of great importance, as it would give rise to new possibilities with regards to quantum technologies. Hybrid entanglement generation has been realized experimentally as well [27].

Here, we discuss the generation of hybrid entangled states that can be generated in DTQW's. Several different approaches to enhance the entanglement between the walker and coin have been explored. A methodical study of the entanglement properties of disordered quantum walks was carried out in Ref. [28]. It was shown that randomly choosing the coin operator at each time step of the quantum walk can lead to maximally entangled states in the asymptotic limit independent of the initial state but only one initial state was analyzed. The effect of the introduction of different types of disorder in the generation of high entangled states was further studied using several numerical experiments [29, 30]. However, this strategy requires a large number of steps to reach the asymptotic limit which is disadvantageous for current experiments. Gratsea, et. al., suggested the optimization of the coin operator sequence using a basin-hopping algorithm[24]. It was shown that maximal entanglement is achieved in just 10 steps. The small number of steps used meant that the experimental challenge of reaching the asymptotic limit was solved. However, the experi-

---

\* bvarun.govind@niser.ac.in

† colin.nano@gmail.com

mental implementation requires potentially the full set of possible coin operators. Recently, two new approaches were proposed in [31]. The first approach presented an entangling sequence (Universal entangler) consisting of a deterministic sequence of Hadamard and Fourier coin operators that created a universal amount of entanglement for a class of localized initial states with vanishing relative phase. This sequence had the disadvantage of only working for an odd number of steps. The second method was based on direct optimization of the coin sequence using reinforcement learning (RL), which is a technique that allows us to determine longer sequences (Optimal entanglers) where brute force optimization is not possible. Although it was shown that optimal sequences were better entanglers than universal entangler, they were highly dependent on initial states.

Our main motivation in this work is to exploit the strategy of turning two unfavorable situations into a favorable one to generate hybrid highly entangled states in discrete-time quantum walks. We propose to use deterministic Parrondo sequences using two different coin operators to produce states that are, in general, more entangled than the states produced by sequences using only one of the two coins. We show that some of the deterministic sequences proposed, apart from generating highly entangled states, generate entanglement that are independent of the phase of the initial state used. We also show that phase independent entangling sequences generate maximally entangled states for 3 and 5 steps regardless of initial states. This could resolve the experimental challenges of generating these states. Further, we explore the asymptotic limit of the sequences proposed. So far, the only study that analyzes the relationships between Parrondo's games and quantum entanglement is Ref. [32]. Winning and losing Parrondo games are defined as in [22], and the winning Parrondo's games are shown to generate good amount of entanglement. However, only two initial states are explored ( $\theta = 0, \phi = \pi/2$  and  $\theta = 0, \phi = 3\pi/2$ ), and the sequences which possess maximum winning outcomes are not the best entanglers.

The paper is organized as follows. In the theory section, we briefly review DTQW's and discuss how the Schmidt Norm can be used as a measure of entanglement. We then introduce Parrondo sequences. In the results section, we present and analyze various Parrondo sequences as regards their propensity to generate highly entangled states. Finally, in the conclusion, we compare our results with other relevant works.

## II. THEORY

### A. Discrete time quantum walks

DTQW's in 1D are defined on a tensor product of two Hilbert spaces  $H = H_P \otimes H_C$ .  $H_C$  represents the 2 dimensional Hilbert space associated with the coin or qubit, whose computational basis is  $\{|0_c\rangle, |1_c\rangle\}$  and  $H_P$

represents the infinite dimensional space associated with the position of the walker, whose computational basis is  $\{|n_p\rangle : n_p \in \mathbb{Z}\}$ . The walker is assumed to be initially localized at position '0' in a general superposition of coin states,

$$|coin\rangle_0 = \cos(\theta/2) |0_p 0_c\rangle + e^{i\phi} \sin(\theta/2) |0_p 1_c\rangle, \quad (1)$$

where  $\theta \in [0, \pi]$  and  $\phi \in [0, 2\pi]$ . The shift is described by an unitary operator, called shift operator

$$S = \sum_{j=-\infty}^{\infty} (|(j+1)_p\rangle \langle j_p| \otimes |0_c\rangle \langle 1_c| + |(j-1)_p\rangle \langle j_p| \otimes |1_c\rangle \langle 0_c|), \quad (2)$$

and the unitary coin operator is

$$C(\alpha, \beta, \gamma, \eta) = e^{i\eta/2} \begin{pmatrix} e^{i\alpha} \cos \beta & e^{i\gamma} \sin \beta \\ -e^{-i\gamma} \sin \beta & e^{-i\alpha} \cos \beta \end{pmatrix}. \quad (3)$$

The full evolution then can then be described as

$$U(t) = S.C(\alpha(t), \beta(t), \gamma(t), \eta(t)). \quad (4)$$

The time evolution of the system after  $t$  steps is then

$$\begin{aligned} |\psi_t\rangle &= U(t) |\psi_{t-1}\rangle = U(t)U(t-1)\dots U(1) |\psi_0\rangle \\ &= \sum_{j=-\infty}^{\infty} [a_1(j, t) |j_p, 0_c\rangle + a_2(j, t) |j_p, 1_c\rangle]. \end{aligned} \quad (5)$$

where,  $a_1(j, t), a_2(j, t)$  are amplitudes of states:  $|j_p, 0_c\rangle$  and  $|j_p, 1_c\rangle$  respectively.

### B. Measure of Entanglement

Entanglement measures quantify the amount of entanglement in a quantum state. There are several measures of entanglement like concurrence[33], logarithmic negativity[34], von Neumann entropy[35]. Here, we use Schmidt Norm as a measure of entanglement[24]. In this work, the total initial state is always pure and the state evolves unitarily, thus it remains a pure state at any later time too. This fact allows us to write the density operator  $\rho$  of  $|\psi\rangle$  directly as  $\rho = |\psi\rangle \langle \psi|$ . As a consequence of singular value decomposition, the normalized state  $|\psi\rangle$  can be re-expressed in a Schmidt-decomposed form[36],

$$|\psi\rangle = \sum_{i=1}^k \lambda_i |\psi_i\rangle_P \otimes |\psi_i\rangle_C, \quad (6)$$

with orthonormal Schmidt vectors  $|\psi_i\rangle_P \in H_P, |\psi_i\rangle_C \in H_C$  and real non-negative Schmidt coefficients  $\lambda_i$  satisfying the normalization condition  $\sum_{i=1}^k |\lambda_i|^2 = 1$  and  $\lambda_1 \geq \lambda_2 \geq \dots \geq \lambda_k \geq 0$  where  $k \leq \min(d_P, d_C)$  is written in terms of dimensions  $d_P$  and  $d_C$  of the position and coin space. The reduced density operator for the coin

space is defined by  $\rho_C \equiv \text{tr}_p(\rho)$  where  $\text{tr}_p$  is the partial trace over the position space. This gives

$$\rho_C = \alpha(t) |0\rangle \langle 0| + \beta(t) |1\rangle \langle 1| + \gamma(t) |0\rangle \langle 1| + \gamma^*(t) |1\rangle \langle 0|, \quad (7)$$

wherein  $\alpha(t) = \sum_{j=-\infty}^{\infty} |a_1(j, t)|^2$ ,  $\beta(t) = \sum_{j=-\infty}^{\infty} |a_2(j, t)|^2$  and  $\gamma(t) = \sum_{j=-\infty}^{\infty} a_1(j, t) a_2^*(j, t)$ . The Schmidt norm[37] is defined as

$$\|\psi\|_{z,k} = \left( \sum_{i=1}^k (\lambda_i)^z \right)^{1/z}. \quad (8)$$

Setting  $z = 1$ , and for the system considered,  $k = \min(d_P, d_C) = 2$ . The Schmidt norm for a maximally entangled state is  $\sqrt{2}$ , since  $\lambda_i = 1/\sqrt{k} = 1/\sqrt{2}$ . Schmidt norm is calculated analytically using the relation between Schmidt coefficients and eigenvalues of the reduced density matrix, see[24]. The reduced density matrix is given as

$$\rho_C = \text{Tr}_p(\rho) = \frac{I}{2} + \vec{n} \cdot \vec{\sigma}. \quad (9)$$

The trace in Eq. (9) is taken over position degrees of freedom.  $I$  is the identity matrix,  $\vec{\sigma}$  is the Pauli vector and

$$\vec{n} = \left( \text{Re}(\sum_j a_1(j, t) a_2^*(j, t)), \text{Im}(\sum_j a_1(j, t) a_2^*(j, t)), \frac{1}{2} \sum_j |a_1(j, t)|^2 - |a_2(j, t)|^2 \right) \quad (10)$$

The eigenvalues of reduced density matrix ( $\rho_C$ ) is then given by

$$E_{\pm} = \frac{1}{2} \pm \sqrt{\frac{1}{4} - \alpha(t)(1 - \alpha(t)) + |\gamma(t)|^2} = \frac{1}{2} \pm |n|. \quad (11)$$

From the identity  $E_{\pm} = \lambda_{\pm}^2$ , one can rewrite the Schmidt norm as

$$S = \|\psi\|_{1,2} = \sqrt{E_-} + \sqrt{E_+}. \quad (12)$$

### C. Parrondo sequences

Parrondo's paradox states that one can strategize to turn two unfavorable strategies into a favorable one by combining them in the right way. We can categorize Parrondo sequences in DTQW's into three categories: (1) Deterministic sequences- the coin used at each step is completely specified before starting the sequence of coins. (2) Random sequences- the coin to be used at each time step is decided randomly. Adaptive sequences- the coin to be used at each time step is decided based on some criterion as the walk proceeds. Our motivation is to generate highly hybrid entangled states by using deterministic Parrondo sequences. We are interested in both small number of time steps as well as in the asymptotic setting of a large number of time steps.

## III. RESULTS

We restrict ourselves to a set of coin operators, Eq. 3: the Hadamard coin  $H = C(\alpha = -\pi/2, \beta = \pi/4, \gamma = -\pi/2, \eta = \pi)$ , the Fourier coin  $F = C(\alpha = 0, \beta = \pi/4, \gamma = \pi/2, \eta = 0)$ , the Miracle coin  $M = C(\alpha = \pi/2, \beta = \pi/4, \gamma = 0, \eta = 0)$ , the flip or Grover coin  $X = C(\alpha \in [0, \pi/2], \beta = \pi/2, \gamma = -\pi/2, \eta = \pi)$ , which have the explicit forms

$$H = \frac{1}{\sqrt{2}} \begin{pmatrix} 1 & 1 \\ 1 & -1 \end{pmatrix}, \quad F = \frac{1}{\sqrt{2}} \begin{pmatrix} 1 & i \\ i & 1 \end{pmatrix}, \quad (13)$$

$$M = \frac{1}{\sqrt{2}} \begin{pmatrix} i & 1 \\ -1 & -i \end{pmatrix}, \quad X = \begin{pmatrix} 0 & 1 \\ 1 & 0 \end{pmatrix}.$$

With these coins, we performed several numerical experiments by forming various deterministic sequences like  $ABAB\dots, BAABAA\dots, AABAAB\dots$ , etc. The primary idea was of finding sequences involving two coins that can perform better than sequences formed using only either of the coins ( $AAA\dots$  and  $BBB\dots$ ). Based on the experiments, we narrowed down to a few better performing sequences.

### A. Parrondo Sequence- $AABAAB\dots$

The first set of sequences we discuss are of the type  $AABAAB\dots$ . We first focus on the cases where  $A$  is always the flip coin  $X$  and  $B$  can be Hadamard coin  $H$  or Fourier coin  $F$  or Miracle coin  $M$ . Fig. 1(a) shows the plot of Schmidt norm  $S$  as a function of number of time steps  $t$  after evolution with the sequences  $XXH\dots, HHH\dots$  and  $XXX\dots$  for  $t = 200$  time steps. Each point is an average over 100 random initial states, randomised in both  $\theta$  and  $\phi$ . The data points are fitted using logarithmic fit and extrapolated to 400 time steps. The existence of Parrondo strategies is evident from Figure 1 for both small number of time steps and in the asymptotic setting. Sequences  $XXF\dots$  and  $XXM\dots$  produced results identical to  $XXH\dots$ . This fact is verified from the equivalence of the analytical expressions of Schmidt norm in terms of the initial state parameters  $\phi$  and  $\theta$  for all  $XXH\dots, XXF\dots$  and  $XXM\dots$ . For the first six steps, the expression for Schmidt norm is given as follows

$$\begin{aligned} \text{After 1 step} &\rightarrow \frac{1}{\sqrt{2}} (\sqrt{1 - \cos(\theta)} + \sqrt{1 + \cos(\theta)}), \\ \text{After 2 steps} &\rightarrow \frac{1}{\sqrt{2}} (\sqrt{1 - \cos(\theta)} + \sqrt{1 + \cos(\theta)}), \\ \text{After 3 steps} &\rightarrow \sqrt{2}, \\ \text{After 4 steps} &\rightarrow \frac{1}{2} \left( \sqrt{2 + \sin(\theta)} + \sqrt{2 - \sin(\theta)} \right), \\ \text{After 5 steps} &\rightarrow \sqrt{2}, \\ \text{After 6 steps} &\rightarrow \frac{1}{2\sqrt{2}} (\sqrt{4 + \sin(\theta)} + \sqrt{4 - \sin(\theta)}). \end{aligned} \quad (14)$$

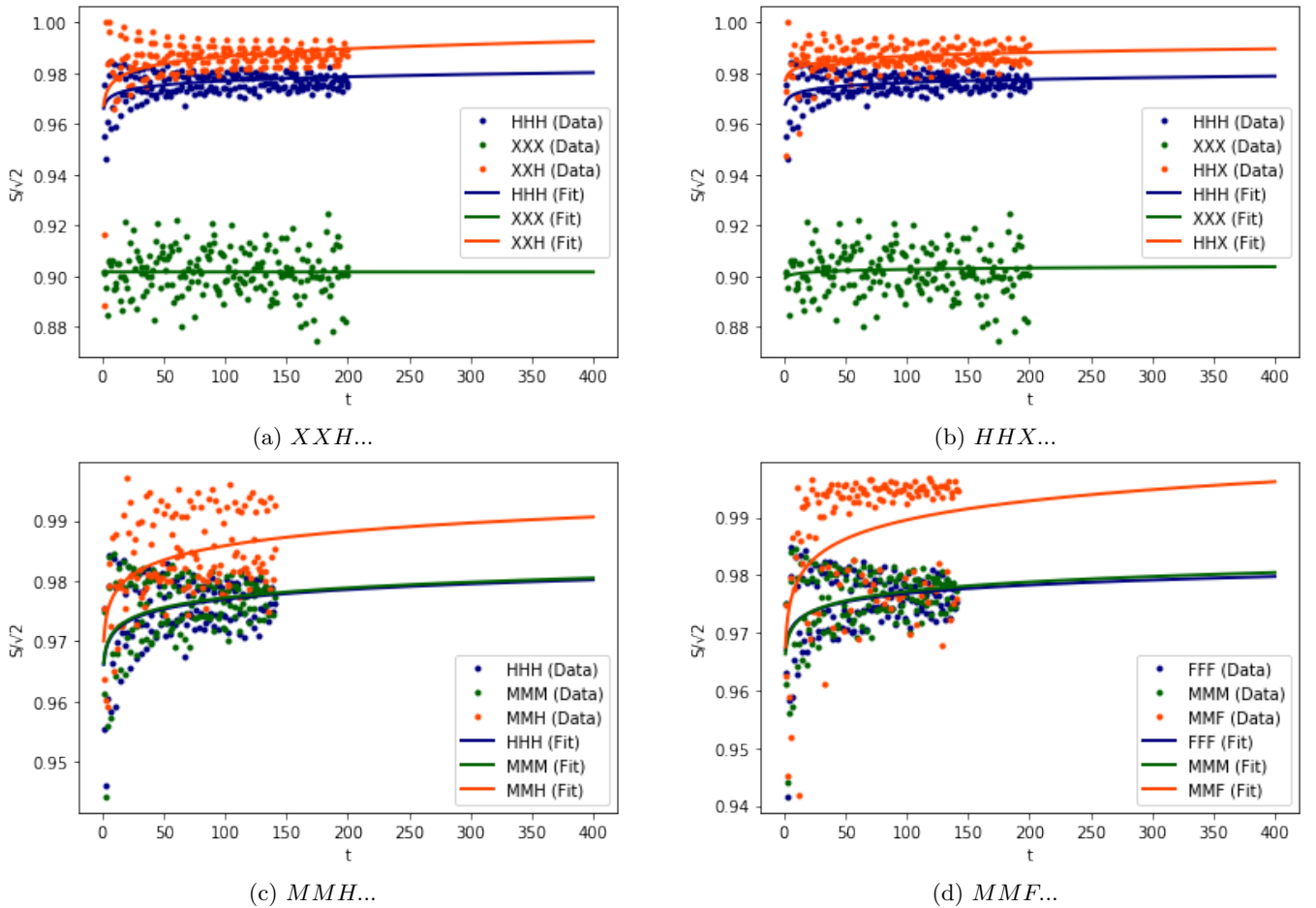


FIG. 1. (a) Schmidt norm  $S$  after evolution with the deterministic Parrondo sequence  $XXH\dots$ . The plots for  $XXF\dots$  and  $XXM\dots$  were found to produce similar results. Schmidt norm  $S$  after evolution with the deterministic Parrondo sequence of the type  $AAB\dots$ . (b)  $HXX\dots$  for 200 time steps. (c)  $MMH\dots$  for 140 time steps. (d)  $MMF\dots$  for 140 time steps. Each point is an average over 100 random initial states, randomised in both  $\theta$  and  $\phi$ .

The analytical expressions reveal that at each step, the value of entanglement  $S$  is independent of the phase  $\phi$ . Due to this property, we refer to the sequences  $XXH\dots$ ,  $XXF\dots$  and  $XXM\dots$  as phase independent entanglers. It is seen from the above expressions that the phase independent entanglers generate maximally entangled states for  $t = 3$  and  $t = 5$  step DTQW's for all initial states. Now, we propose some more Parrondo sequences that belong to  $AABAAB\dots$  type. Fig. 1(b-d) show the plots of Schmidt norm  $S$  as a function of number of time steps  $t$  after evolution with sequences  $HXX\dots$  for 200 time steps,  $MMH\dots$  for 140 time steps and  $MMF\dots$  for 140 time steps. Due to high computational cost, the steps were reduced in some of the experiments. Each point is an average over 100 random initial states, randomised in both  $\theta$  and  $\phi$ . The data points are fitted using logarithmic fit and extrapolated to 400 time steps. In all the cases, a good enhancement in entanglement is seen. It has to be noted that the results of Parrondo sequences  $FFX\dots$ ,  $HMM\dots$ ,  $FFM\dots$  are similar to  $HXX\dots$ ,  $MMH\dots$ ,  $MMF\dots$  respectively when a

large number of random initial states are considered and averaged. This again can be attributed to the fact that  $F$  and  $M$  act as phase shifted  $H$ . Also, it is to be noted that the above sequences are not phase independent entanglers.

Figure 2(a) shows the Schmidt norm as a function of the initial state parameters  $\theta$  and  $\phi$  for the phase independent entanglers, again verifying the independence of phase  $\phi$  in the value of entanglement  $S$ . In order to gain further insight, the plots of Schmidt norm as function of the initial state parameters  $\theta$  and  $\phi$  for sequences  $HHH\dots$ ,  $FFF\dots$  and  $MMM\dots$  are shown in Fig. 2(b-d). A simple comparison between the Schmidt norm plots for  $HHH\dots$ ,  $FFF\dots$  and  $MMM\dots$  tells us that the sequences  $FFF\dots$  and  $MMM\dots$  generate values of  $S$  that are shifted by a phase of  $-\pi/2$  and  $+\pi/2$  respectively with respect to the value of  $S$  generated by  $HHH\dots$ . This fact can be further verified by comparing the analytical expressions of  $S$  as a function of  $\theta$  and  $\phi$  for the sequences  $HHH\dots$ ,  $FFF\dots$  and  $MMM\dots$ . For example, consider the analytical expressions of  $S$  in the form  $\sqrt{E_-} + \sqrt{E_+}$  for

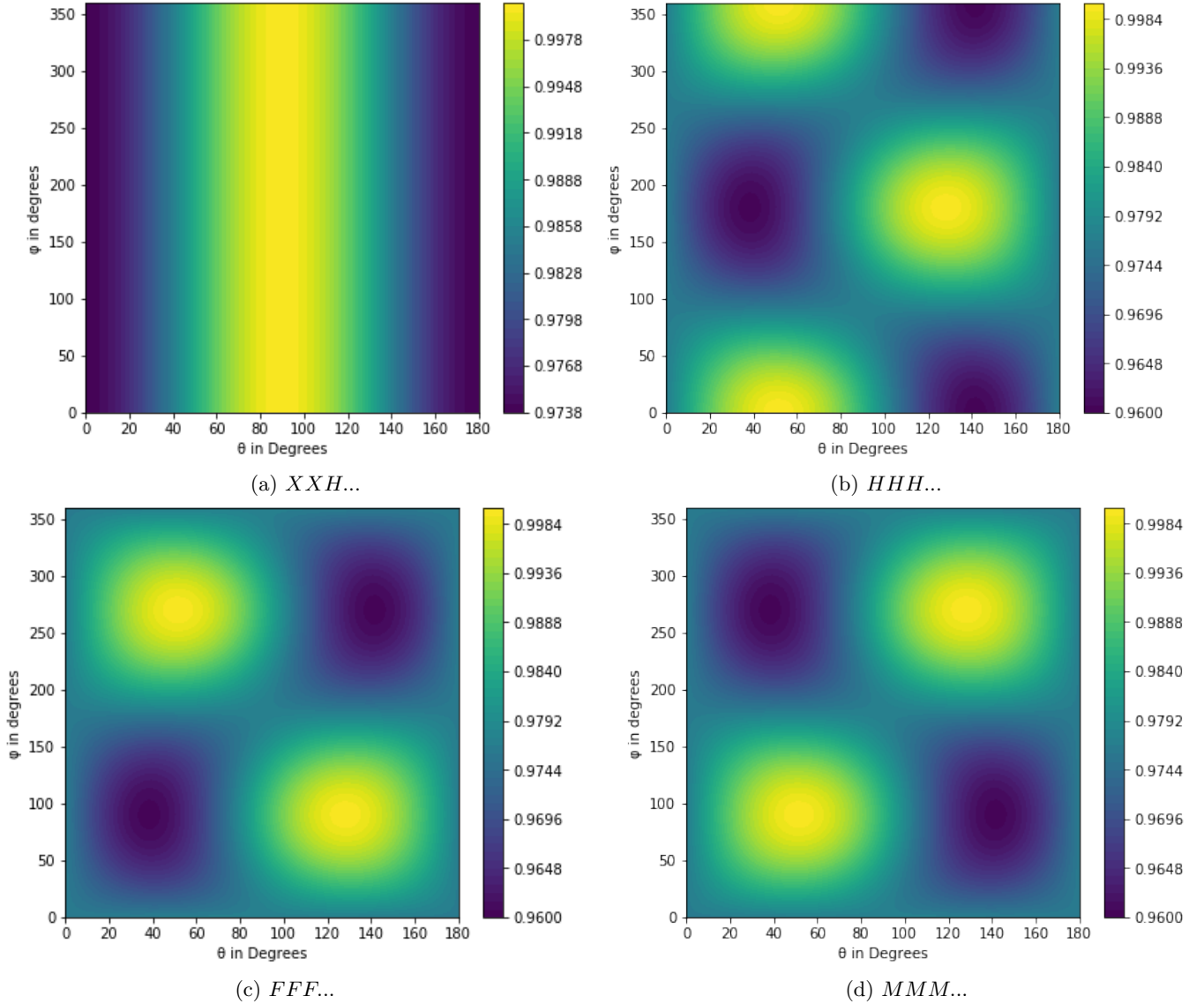


FIG. 2. (a) Contour plot of Schmidt norm as a function of the initial state parameters  $\phi$  and  $\theta$  for  $XXH\dots$  for a 50 time step DTQW. The contour plots for  $XXF\dots$  and  $XXM\dots$  were found to be identical to that of  $XXH\dots$ . Contour plots of Schmidt norm as a function of the initial state parameters  $\phi$  and  $\theta$  for (b)  $HHH\dots$  (c)  $FFF\dots$  and (d)  $MMM\dots$  for 50 time steps.

a single step DTQW evolved using  $H$ , or  $F$  or  $M$ ,

$$\begin{aligned}
 H &\rightarrow \frac{1}{\sqrt{2}}(\sqrt{1 + \sin(\theta) \cos(\phi)} + \sqrt{1 - \sin(\theta) \cos(\phi)}) \\
 F &\rightarrow \frac{1}{\sqrt{2}}(\sqrt{1 + \sin(\theta) \sin(\phi)} + \sqrt{1 - \sin(\theta) \sin(\phi)}) \\
 M &\rightarrow \frac{1}{\sqrt{2}}(\sqrt{1 - \sin(\theta) \sin(\phi)} + \sqrt{1 + \sin(\theta) \sin(\phi)})
 \end{aligned}
 \tag{15}$$

Substituting the identities  $\cos(\phi - \pi/2) = \sin(\phi)$  and  $\cos(\phi + \pi/2) = -\sin(\phi)$  in the analytical expression of  $S$  for  $H$  verifies this assertion. The same fact can be verified for any time step  $t$ . Hence, the similarity in results between  $XXH\dots$ ,  $XXF\dots$  and  $XXM\dots$  can be attributed

to the fact that the fourier coin  $F$  and the miracle coin  $M$  act like phase shifted Hadamard coin  $H$  when considered in terms of entanglement generation.

### B. Parrondo sequence- $ABBABB\dots$

Fig. 3 shows the plots of Schmidt norm  $S$  as a function of number of time steps  $t$  after evolution with the sequence  $XHH\dots$ . Here again, a good enhancement in entanglement for  $XHH\dots$  is seen in comparison to  $HHH\dots$  and  $XXX\dots$ . Here too, a similarity between the results of  $XHH\dots$  and  $FFF\dots$  was found. However, the results of  $XMM$  aren't as good as  $XHH$  and  $FFF$ . The exact

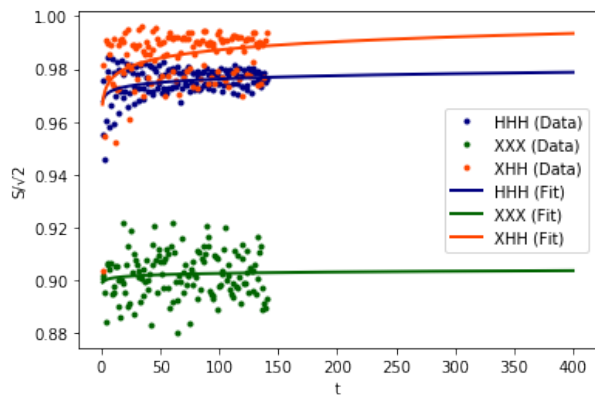


FIG. 3. Schmidt norm  $S$  after evolution with the deterministic Parrondo sequence  $XHH\dots$  for 140 time steps. Each point is an average over 100 random initial states, randomised in both  $\theta$  and  $\phi$ . The sequence  $FFF\dots$  was found to produce similar results.

reason requires further study.

### C. Parrondo sequence- $ABAB\dots$

Fig. 4 shows the plots of Schmidt norm  $S$  as a function of the number of time steps  $t$  after evolution with sequences  $XHXH\dots, HXHX\dots$ . Sequences  $XHXH\dots, FXFX\dots$  and  $MXMX\dots$  generate similar results while sequences  $HXHX\dots, FXFX\dots$  and  $MXMX\dots$  generate similar results. As in the previous sections, this can be reasoned as a manifestation of the relation between  $H, F$  and  $M$ .

## IV. DISCUSSION AND CONCLUSION

Finally, we compare the various Parrondo sequences suggested above in Figure 5. It has already been seen that when each point is averaged for a large number of states, the plots for some of the cases within a specific sequence produce similar results. Sequences with similar results have been grouped together in figure 5. Fig. 5 (a) suggests that, for any small time step we could find coin sequences that yield high average values of entanglement over a large number of initial states, which is particularly useful in cases where the initial state is not fully known, very noisy, or simply whenever it is required to generate highly entangled states independent of the initial state [31]. In Fig. 5(b), we compare the results in the asymptotic setting. Using data points of 140 time steps for each sequence, the logarithmic fit was extrapolated to 400 time steps.  $MMF\dots$  and  $FFM\dots$  seem to produce the best results when large number of steps are considered,  $S/\sqrt{2} = 0.9962$  at the 400th time step. The exact asymptotic value for each sequences requires further experimentation. The central goal in this

work was to show that deterministic Parrondo strategies can generate highly entangled states when implemented on DTQW's. Using Schmidt norm as the measure of entanglement, we showed that several deterministic sequences formed using two coin operators were better entanglers than single coined-sequences made of either one of the two coins. We also showed that the Parrondo sequences  $XXH\dots, XXF\dots$  and  $XXM\dots$ , generate entanglement that is independent of the phase of the initial state used. Furthermore, we showed  $XXF\dots, XXH\dots$  and  $XXM\dots$ , generate maximally entangled states for 3 and 5 step quantum walks for all initial states. A comparison between various Parrondo sequences showed that when each point is averaged for a large number of states, the plots of some of the sequences within a type of strategy (like  $ABAAB\dots, ABAB\dots$ ) produce similar results. The similarities in results were understood to be associated with the fact that the Fourier coin  $F$  and the miracle coin  $M$  act like phase shifted Hadamard coin  $H$  when considered in terms of entanglement generation. The comparison also suggested that, for any number of time steps  $t$ , one could find coin sequences that yield high average values of entanglement for a large number of initial states. This is advantageous in cases where the initial state is not fully known, very noisy, or simply whenever it is required to generate highly entangled states independent of the initial state[31]. It was also seen that the strategies displayed Parrondo's paradox even when large number of steps are considered. Finally, we compare our results with the previous works [24, 29–31]. Fig. 6 shows a comparison plot between Parrondo strategies and optimal entanglers [31]. Schmidt norm  $S$  was plotted for 3, 5, 7, 15 step DTQW's. Each data point was obtained after averaging over 1000 random initial states, randomised in both  $\theta$  and  $\phi$ . The plot shows that Parrondo strategies  $XXH\dots, XXF\dots$  and  $XXM\dots$  produce higher values of entanglement ( $S$ ) than Optimal entanglers for 3, 5, 15 step quantum walks.  $XHH$  produces higher values of entanglement for steps 5 and 7 in comparison to optimal entanglers. Also,  $XXH\dots, XXF\dots, XXM\dots$  give maximally entangled states ( $S/\sqrt{2} = 1$ ) regardless of the initial state used for 3 and 5 step quantum walks. This is valuable for an experimental setting where the number of possible steps should be as minimum as possible. This serves as an example for cases where we should find coin sequences that yield high average values of entanglement over a large number of initial states for a given  $t$ - time step quantum walk. This is important in an experimental setting where the initial state/states is not fully known [31]. As a conclusion, we compare our best results with all the other works [24, 29–31] discussed focusing on the similarities and differences among them in Table I. As a conclusion, we compare our best results with some other works [24, 29–31] discussed focusing on the similarities and differences among them in Table I. The first comparison we make is of the type of sequences used. We used deterministic sequences as opposed to Vieira, et. al. [29, 30], where disordered sequences are

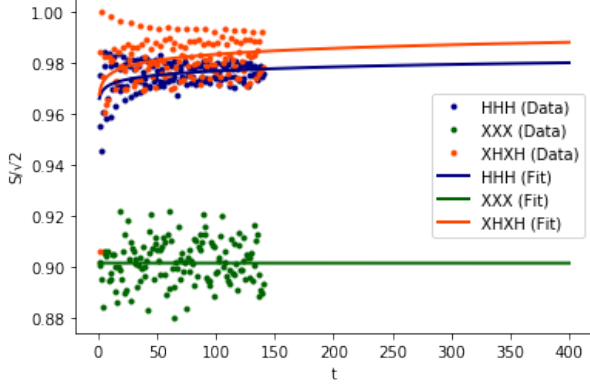
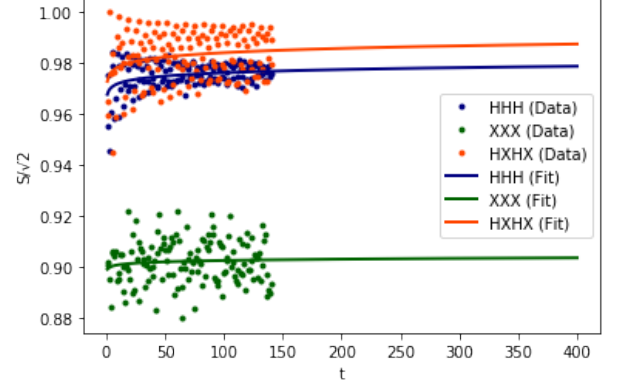
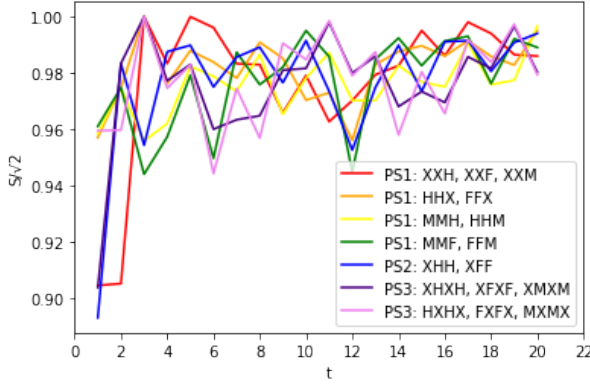
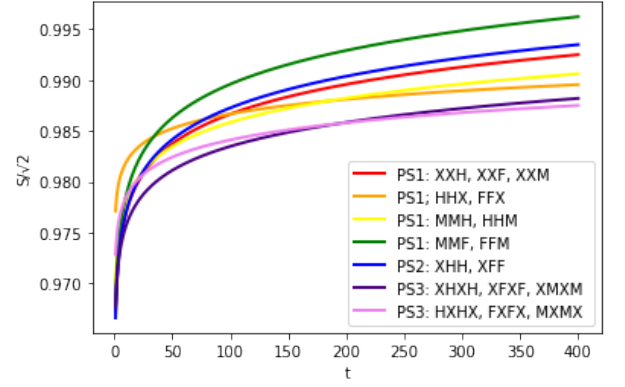
(a)  $XHXH\dots$ (b)  $HXHX\dots$ 

FIG. 4. Schmidt norm  $S$  after evolution with Parrondo sequence of type  $ABAB\dots$  for 140 time steps. Each point is an average over 100 random initial states, randomised in both  $\theta$  and  $\phi$ . The data points are fitted using logarithmic fit and extrapolated to 400 time steps.



(a)



(b)

FIG. 5. Comparison between various Parrondo sequences.  $PS1 = AABAAB\dots$ ,  $PS2 = ABBABB\dots$ ,  $PS3 = ABAB\dots$  a) For small number of steps. Each point is an average of 1000 random initial states, randomised in both  $\theta$  and  $\phi$ . The data points of 140 step DTQW (each point is an average over 100 random initial states, randomised in both  $\theta$  and  $\phi$ .) are fitted using logarithmic fit and extrapolated to 400 time steps.

TABLE I. Comparison between various approaches

Properties↓/Model→	DTQW with Parrondo sequences (This paper)	DTQW with disorder Refs. [29, 30]	DTQW with Optimization (basin hopping algorithm) Ref. [24]	DTQW with Optimization (Reinforcement Learning technique) Ref. [31]
<b>Dependence of Entanglement on initial state parameters</b>	Independent of phase $\phi$ for XXH..., XXM... and XXF...	Asymptotic limit was shown to be independent of initial parameters	$\theta$ and $\phi$ dependent	Universal Entangler: $\theta$ independent for $\phi = 0$ states Optimal Entangler: $\theta$ and $\phi$ dependent
<b>No of coins used</b>	2 coins per sequence	2 coins in $RQ\overline{R}W_2$ , full set of possible coins in $RQ\overline{R}W_\infty$	Full set of possible coins	2 coins
<b>5 steps</b>	Maximal Entanglement.	Not discussed.	Around 98% entanglement.	Optimal entangler range: 0.968 – 0.999
<b>20 steps</b>	Maximum average value for MMH..., HHM...: $S/\sqrt{2} = 0.997$ See Fig. 1(c)	Not discussed	Not discussed	Not discussed
<b>Asymptotic limit</b>	Based on logarithmic fit, all Parrondo sequences give entanglement $S/\sqrt{2} = 0.985$ and above in the asymptotic limit. Sequences MMF...and FFM...produced the best result, $S/\sqrt{2} = 0.9962$ at the 400th time step. See Fig. 1(d)	Achieves Maximal entanglement at large number of steps.	Not calculated	Not calculated

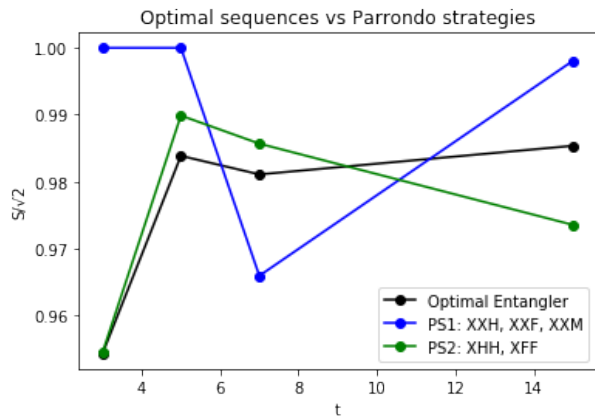


FIG. 6. Parrondo sequences v Optimal entanglers (see Gratsea, et. al.,[31]). Schmidt norm  $S$  plotted for 3, 5, 7, 15 step quantum walks. Each point is an average over 1000 random initial states (randomised in both  $\theta$  and  $\phi$ )

used. Gratsea et al., mainly focus on optimisation to find sequences, but also propose one deterministic sequence - Universal entangler. The independence of entanglement value from initial state parameter  $\phi$  for all states and for any time step is a unique feature seen only in  $XXH..$ ,  $XXF..$ ,  $XXM..$  Parrondo sequences. For initial states with  $\phi = 0$ ,  $\theta$  independence is observed for Universal entanglers for any time step. In the asymptotic limit, disordered sequences discussed by Vieira, et. al., produced maximal entanglement irrespective of the

initial state parameters. Another important property to be considered is the number of coin operators used, as lesser the coins the easier is the experimental realization. In terms of this property, Parrondo sequences are as good as the universal and optimal entanglers[31], and  $RQRW_2$ [29, 30]. Gratsea, et. al.[31], focus only on small number of time steps. In their first paper, it was shown that maximal entanglement is achieved in just 10 steps. Optimal entangler generates entanglement in the range of 0.968 – 0.999 for 5–time steps, but Parrondo sequences  $XXH..$ ,  $XXF..$ ,  $XXM..$  gives maximal entanglement. The case of small number of time steps is not discussed in Refs. [29, 30]. In the asymptotic limit, Vieira, et. al.[29, 30], showed that disordered sequences achieve maximal entanglement. On using logarithmic fit, Parrondo sequences  $MMF..$  and  $FFM..$  produced the best result,  $S/\sqrt{2} = 0.9962$  at the 400th time step.

## ACKNOWLEDGMENTS

Colin Benjamin would like to thank Science and Engineering Research Board (SERB) for funding under MATRICS grant "Nash equilibrium versus Pareto optimality in N-Player games" (MTR/2018/000070) and under Core Research grant "Josephson junctions with strained Dirac materials and their application in quantum information processing", Grant No. CRG/2019/006258.

## V. APPENDIX

The following python code is written based on [38] and gives the data points for the sequence  $XXH..$  in figure 1(a). The data points were later fitted using logarithmic fit.

```

from numpy import *
from matplotlib.pyplot import *
N =400# number of random steps
S400 = empty(N+1)
for m in range(1, N + 1):
    P = 2*m+1 # number of positions
    coin0 = array([1, 0]) # |0>
    coin1 = array([0, 1]) # |1>
    C00 = outer(coin0, coin0) # |0><0|
    C01 = outer(coin0, coin1) # |0><1|
    C10 = outer(coin1, coin0) # |1><0|
    C11 = outer(coin1, coin1) # |1><1|
    S = 0
    for g in range(0, 100): #100 random initial states
        C_hat = (cos(radians(45))*C00 + sin(radians(45))*C01 + sin(radians(45))*C10 - cos(radians(45))*C11) #Hadamard coin
        K_hat = (0*C00 + 1*C01 + 1*C10 + 0*C11) #Grover coin
        F_hat = (C00 + 1j*C01 + 1j*C10 + C11)/sqrt(2.) #Fourier coin
        M_hat = (1j*C00 + C01 - C10 - 1j*C11)/sqrt(2.) #Miracle coin
        ShiftPlus = roll(eye(P), 1, axis=0)
        ShiftMinus = roll(eye(P), -1, axis=0)
        S_hat = kron(ShiftPlus, C01) + kron(ShiftMinus, C10)
        H = S_hat.dot(kron(eye(P), C_hat)) #Hadamard coin plus shift
        X = S_hat.dot(kron(eye(P), K_hat)) #Grover coin plus shift
        F = S_hat.dot(kron(eye(P), F_hat)) #Fourier coin plus shift
        M = S_hat.dot(kron(eye(P), M_hat)) #Miracle coin plus shift
        posn0 = zeros(P)
        posn0[m] = 1
        l = random.randint(0, 180)
        phi = random.randint(0, 360)
        psi0 = kron(posn0, (cos(radians(l/2))*coin0 + exp(1j*radians(phi))*sin(radians(l/2))*coin1))
        psiN = psi0 # Initialisation

```

```

for i in range(1, m + 1):
    if (i)%3==0:
        psiN = linalg.matrix_power(X, 1).dot(psiN) #B
    else:
        psiN = linalg.matrix_power(H, 1).dot(psiN) #AA
prob1 = empty(P)
prob2 = empty(P)
prob3 = empty(P)
prob = empty(P)
for k in range(P):
    posn = zeros(P)
    posn[k] = 1
    M_hat_k = kron( outer(posn,posn), eye(2))
    X_hat_k = kron( outer(posn,posn), C00)
    W_hat_k = kron( outer(posn,posn), C11)
    proj = M_hat_k.dot(psiN)
    proj1 = X_hat_k.dot(psiN)
    proj01 = X_hat_k.dot(kron(posn,(coin0)))
    proj2 = W_hat_k.dot(psiN)
    proj02 = W_hat_k.dot(kron(posn,(coin1)))
    prob1[k] = (proj02.dot(proj2.conjugate()))*proj01.dot(proj1.conjugate()).conjugate().real
    prob2[k] = (proj02.dot(proj2.conjugate()))*proj01.dot(proj1.conjugate()).conjugate().imag
    prob3[k] = ((proj1.dot(proj1.conjugate()))).real - (proj2.dot(proj2.conjugate()))).real)/2
n1 = n2 = n3 = 0
for j in range(P):
    n1 = prob1[j] + n1
    n2 = prob2[j] + n2
    n3 = prob3[j] + n3
n = sqrt(n1**2 + n2**2 + n3**2)
S = S + sqrt(0.5 - n) + sqrt(0.5 + n)
g = g + 1
S400[m]=S/(100*(sqrt(2)))
print(S400[m])

```

- 
- [1] J. M. R. Parrondo, G. P. Harmer, and D. Abbott, New paradoxical games based on brownian ratchets, *Physical Review Letters* **85**, 52265229 (2000).
- [2] D. Abbott, Developments in Parrondos paradox, in *Applications of Nonlinear Dynamics: Model and Design of Complex Systems*, edited by V. In, P. Longhini, and A. Palacios (Springer Berlin Heidelberg, Berlin, Heidelberg, 2009) pp. 307321.
- [3] Joel Weijia Lai and Kang Hao Cheong, *Nonlinear Dynamics* 100, 849-861 (2020).
- [4] A. Allison and D. Abbott, Control systems with stochastic feedback, *Chaos: An Interdisciplinary Journal of Nonlinear Science* **11**, 715724 (2001).
- [5] A. P. Flitney, Quantum Parrondos games using quantum walks (2012), arXiv:1209.2252 [quant-ph].
- [6] D. A. Meyer, Noisy quantum Parrondo games, *Fluctuations and Noise in Photonics and Quantum Optics* (2003).
- [7] Y. Aharonov, L. Davidovich, and N. Zagury, Quantum random walks, *Physical Review A* 48, 1687-1690 (1993).
- [8] R. PORTUGAL, QUANTUM WALKS AND SEARCH ALGORITHMS (SPRINGER, 2019).
- [9] K. Manouchehri and J. Wang, Quantum random walk with Rb atoms, *Journal of Physics: Conference Series* **185**, 012026 (2009).
- [10] F. Cardano, F. Massa, H. Qassim, E. Karimi, S. Slusarenko, D. Paparo, C. D. Lisio, F. Sciarrino, E. Santamato, R. W. Boyd, and et al., Quantum walks and wave packet dynamics on a lattice with twisted photons, *Science Advances* **1**, 15516 (2015).
- [11] A. Schreiber, K. N. Cassemiro, V. Potocek, A. Gabris, P. J. Mosley, E. Andersson, I. Jex, and C. Silberhorn, Photons walking the line: A quantum walk with adjustable coin operations, *Physical Review Letters* **104**, 050502(2010).
- [12] M. Karski, L. Forster, J.-M. Choi, A. Steffen, W. Alt, D. Meschede, and A. Widera, Quantum walk in position space with single optically trapped atoms, *Science* **325**, 174177 (2009).
- [13] C. Robens, S. Brakhane, D. Meschede, and A. Alberti, Quantum walks with neutral atoms: Quantum interference effects of one and two particles, *Laser Spectroscopy* (2016).
- [14] C. A. Ryan, M. Laforest, J. C. Boileau, and R. Laflamme, Experimental implementation of a discrete-time quantum random walk on an NMR quantum-information processor, *Physical Review A* **72**, 062317 (2005).
- [15] J.-Q. Zhou, L. Cai, Q.-P. Su, and C.-P. Yang, Protocol of a quantum walk in circuit QED, *Physical Review A* **100**, 012343 (2019).
- [16] E. Flurin, V. Ramasesh, S. Hacothen-Gourgy, L. Martin, N. Yao, and I. Siddiqi, Observing topological invariants using quantum walks in superconducting circuits, *Physical Review X* **7** (2017).
- [17] H. Schmitz, R. Matjeschk, C. Schneider, J. Glueckert, M. Enderlein, T. Huber, and T. Schaetz, Quantum walk of a trapped ion in phase space, *Physical Review Letters* **103**, 090504 (2009).
- [18] F. Zahringer, G. Kirchmair, R. Gerritsma, E. Solano, R. Blatt, and C. F. Roos, Realization of a quantum walk with one and two trapped ions, *Physical Review Letters* **104**, 100503 (2010).
- [19] G. Puentes, Topology and holonomy in discrete-time quantum walks, *Crystals* **7**, 122 (2017).
- [20] C. M. Chandrashekar and S. Banerjee, Parrondos game using a discrete-time quantum walk, *Physics Letters A*

- 375**, 1553 (2011).
- [21] L. Neves and G. Puentes, Photonic discrete-time quantum walks and applications, *Entropy* **20**, 731 (2018).
- [22] J. Rajendran and C. Benjamin, Implementing Parrondos paradox with two-coin quantum walks, *Royal Society Open Science* **5**, 171599 (2018).
- [23] J. Rajendran and C. Benjamin, Playing a true Parrondos game with a three-state coin on a quantum walk, *EPL(Europhysics Letters)* **122**, 40004 (2018).
- [24] A. Gratsea, M. Lewenstein, and A. Dauphin, Generation of hybrid maximally entangled states in a one-dimensional quantum walk, *Quantum Science and Technology* **5**, 025002 (2020).
- [25] G. Zhu, L. Xiao, B. Huo, and P. Xue, Photonic discrete-time quantum walks, *Chinese Optics Letters* **18**, 052701 (2020).
- [26] S. Slussarenko and G. J. Pryde, Photonic quantum information processing: A concise review, *Applied Physics Reviews* **6**, 041303 (2019).
- [27] S. Li, H. Yan, Y. He, and H. Wang, Experimentally feasible generation protocol for polarized hybrid entanglement, *Physical Review A* **98**, 022334 (2018).
- [28] C. M. Chandrashekar, Disorder induced localization and enhancement of entanglement in one and two-dimensional quantum walks (2012), arXiv:1212.5984[quant-ph].
- [29] R. Vieira, E. P. M. Amorim, and G. Rigolin, Dynamically disordered quantum walk as a maximal entanglement generator, *Physical Review Letters* **111**, 180503 (2013).
- [30] R. Vieira, E. P. M. Amorim, and G. Rigolin, Entangling power of disordered quantum walks, *Physical Review A* **89**, 042307 (2014).
- [31] A. Gratsea, F. Metz, and T. Busch, Universal and optimal coin sequences for high entanglement generation in 1d discrete time quantum walks (2020), arXiv:2003.07141[quant-ph].
- [32] M. Jan, X.-Y. Xu, W. Q. Qin, W.-W. Pan, Y.-J. Han, C.-F. Li, and G.-C. Guo, Study of Parrondos paradox regions in one-dimensional quantum walks (2020), arXiv:2006.16585 [quant-ph].
- [33] R. Hildebrand, Concurrence revisited, *Journal of Mathematical Physics* **48**, 102108 (2007).
- [34] M. B. Plenio, Logarithmic negativity: A full entanglement monotone that is not convex, *Physical Review Letters* **95**, 090503 (2005)
- [35] D. Janzing, Entropy of entanglement, *Compendium of Quantum Physics*, 205209 (2009).
- [36] R. Reuvers, An algorithm to explore entanglement in small systems, *Proceedings of the Royal Society A: Mathematical, Physical and Engineering Sciences* **474**, 20180023 (2018).
- [37] J. B. Conway, *A course in functional analysis*, Graduate Texts in Mathematics (2007).
- [38] <http://susan-stepney.blogspot.com/2014/02/mathjax.html> (2014).